

Supplement of Atmos. Chem. Phys., 15, 10777–10798, 2015
<http://www.atmos-chem-phys.net/15/10777/2015/>
doi:10.5194/acp-15-10777-2015-supplement
© Author(s) 2015. CC Attribution 3.0 License.



Supplement of

Modelling the contribution of biogenic volatile organic compounds to new particle formation in the Jülich plant atmosphere chamber

P. Roldin et al.

Correspondence to: P. Roldin (pontus.roldin@nuclear.lu.se)

The copyright of individual parts of the supplement might differ from the CC-BY 3.0 licence.

Table S1. The initial VOC gas-phase reaction rates with OH, O₃ and NO₃ used in the model.

Name	$k_{\text{OH}} (\text{cm}^3 \text{s}^{-1})$	$k_{\text{O}_3} (\text{cm}^3 \text{s}^{-1})$	$k_{\text{NO}_3} (\text{cm}^3 \text{s}^{-1})$
Isoprene ξ	$2.7 \times 10^{-11} e^{(390/T) a}$	$1.03 \times 10^{-14} e^{(-1995/T) a}$	$3.15 \times 10^{-12} e^{(-450/T) a}$
α -Pinene ξ	$1.2 \times 10^{-11} e^{(440/T) a}$	$6.3 \times 10^{-16} e^{(-580/T) a}$	$1.2 \times 10^{-12} e^{(490/T) a}$
β -Pinene ξ	$2.38 \times 10^{-11} e^{(357/T) a}$	$1.5 \times 10^{-17} a$	$2.51 \times 10^{-12} a$
Myrcene Ξ	$2.15 \times 10^{-10} b$	$4.7 \times 10^{-16} b$	$1.1 \times 10^{-11} b$
Sabinene Ξ	$1.17 \times 10^{-10} b$	$8.6 \times 10^{-17} b$	$1.0 \times 10^{-11} b$
Camphene Ξ	$5.3 \times 10^{-11} b$	$9.0 \times 10^{-19} b$	$6.6 \times 10^{-13} b$
Ocimene ζ	$2.52 \times 10^{-10} b$	$5.40 \times 10^{-16} b$	$2.2 \times 10^{-11} b$
Δ^3 -Carene α	$8.8 \times 10^{-11} b$	$3.7 \times 10^{-17} b$	$9.1 \times 10^{-12} b$
α -Terpinene Ξ	$3.63 \times 10^{-10} b$	$2.11 \times 10^{-14} b$	$1.4 \times 10^{-10} b$
γ -Terpinene Ξ	$1.77 \times 10^{-10} b$	$1.4 \times 10^{-16} b$	$2.9 \times 10^{-11} b$
α -Phellandrene Ξ	$3.13 \times 10^{-10} b$	$2.98 \times 10^{-15} b$	$8.5 \times 10^{-11} b$
β -Phellandrene Ξ	$1.68 \times 10^{-10} b$	$4.7 \times 10^{-17} b$	$8.0 \times 10^{-12} b$
Terpinolene Ξ	$2.25 \times 10^{-11} b$	$1.88 \times 10^{-15} b$	$9.7 \times 10^{-11} b$
Tricyclene Ξ	$2.86 \times 10^{-12} c$		
Other MTs β	Same as α -Pinene	Same as α -Pinene	Same as α -Pinene
β -Caryophyllene ξ	$1.97 \times 10^{-10} a$	$1.16 \times 10^{-14} a$	$1.9 \times 10^{-11} a$
Farnesene Ξ	Same as β -Caryop.	Same as β -Caryop.	Same as β -Caryop.
α -Longipinene Ξ		$2.9 \times 10^{-16} d$	
Δ -Cardinene Ξ		$3.2 \times 10^{-15} d$	
Other SQTs Ξ	Same as β -Caryop.	Same as β -Caryop.	Same as β -Caryop.
2-Butanol ξ	$8.7 \times 10^{-10} a$		
Hexanal ξ	$2.88 \times 10^{-11} a$		$1.4 \times 10^{-12} e^{(-1860/T) a}$
Benzene ξ	$2.3 \times 10^{-12} e^{(-190/T) a}$		
Toluene ξ	$1.8 \times 10^{-12} e^{(340/T) a}$		
Eucalyptol Ξ	$1.1 \times 10^{-11} e$	$1.5 \times 10^{-19} f$	$1.7 \times 10^{-16} e$
Nonanal Ξ	$3.6 \times 10^{-11} g$		
Bornyl acetate Ξ	$1.39 \times 10^{-11} h$		
Methyl salicylate Ξ	$4.0 \times 10^{-21} i$		

^a Master Chemical Mechanism v 3.2 (Jenkin et al., 1997, 2012; Saunders et al., 2003), ^b Atkinson (1997), ^c Atkinson and Aschmann (1992), ^d Pollmann *et al.* (2005), ^e Corchnoy and Atkinson (1990), ^f Atkinson *et al.* (1990), ^g Bowman *et al.* (2003), ^h Coeur *et al.* (1998), ⁱ Canosa-Mas *et al.* (2002), ξ Full MCMv3.2 chemistry. Ξ Only the initial reactions were represented, not the reactions of the formed oxidation products. ζ Chemistry beyond the first oxidation step was approximated with that of limonene. α Chemistry beyond the first oxidation step was approximated with that of α -pinene. β Chemistry beyond the first oxidation step was approximated with that of α -pinene (50 %) and β -pinene (50 %).

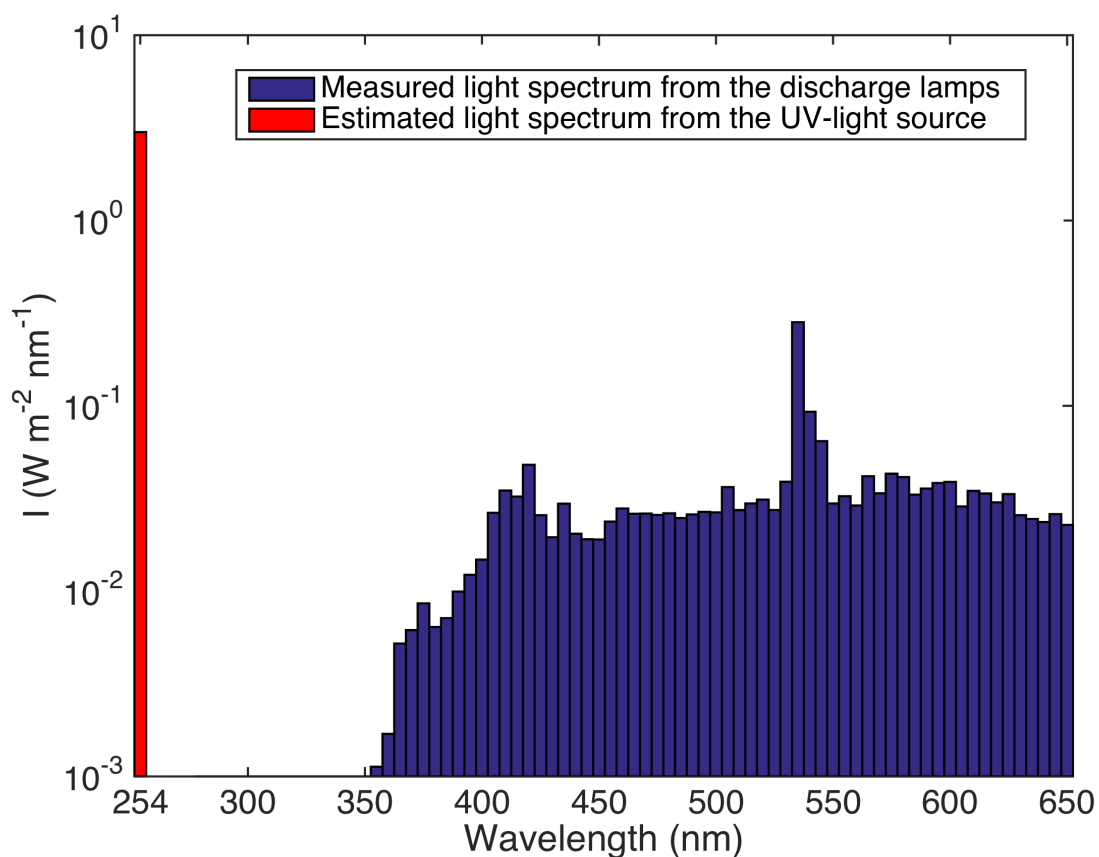


Figure S1. Light spectrum intensity (I) in the reaction chamber. The light spectrum was used to calculate the photolysis rate coefficients used in the MCMv3.2 gas-phase chemistry. The light spectrum has been discretized into 5 nm wavelength intervals. The red bar corresponds to the estimated single 254 nm light spectrum peak from the UV-light source (Philips, TUV 40W lamp).

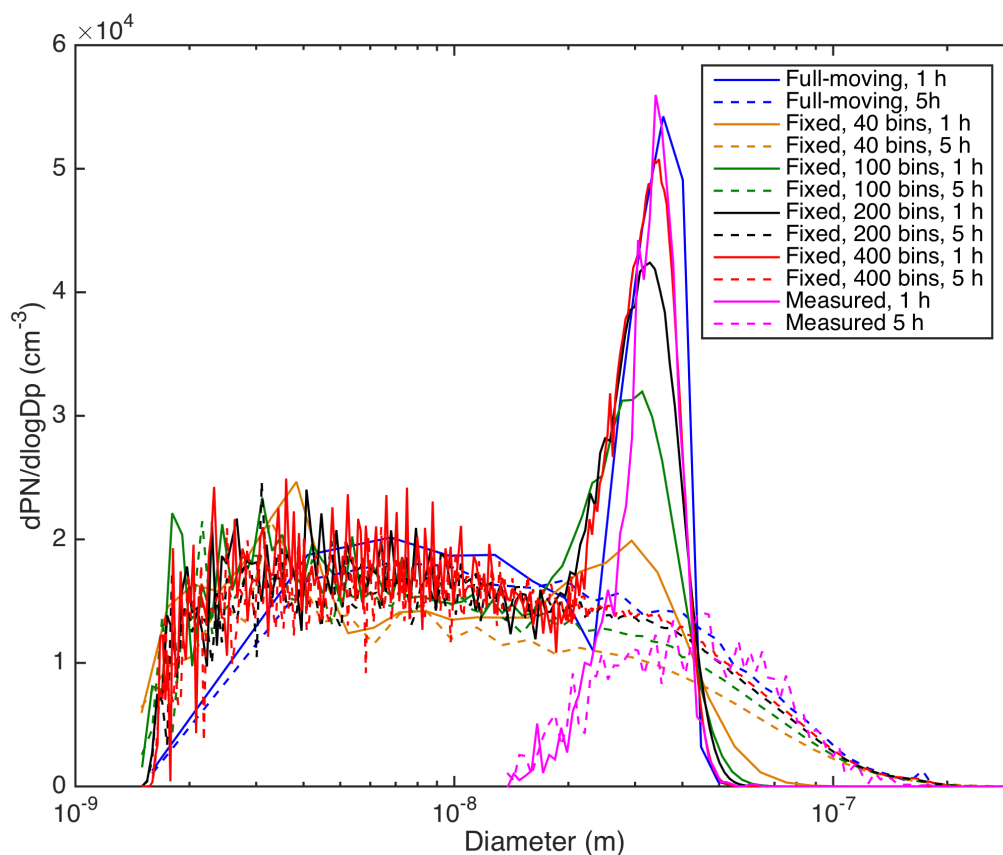


Figure S2. Modelled and measured particle number size distributions during Day-2 at 1 and 5 hours after the UV-lights were turned on, respectively. The simulations were performed with the 2D-VBS ($k_{\text{OH}} = 5 \times 10^{-11} \text{ cm}^3 \text{ s}^{-1}$ and O:C = 0.4 for the first generation oxidation products). The only differences between the different model simulations are the size distribution method used (fixed sections or full-moving) and the number of size bins.

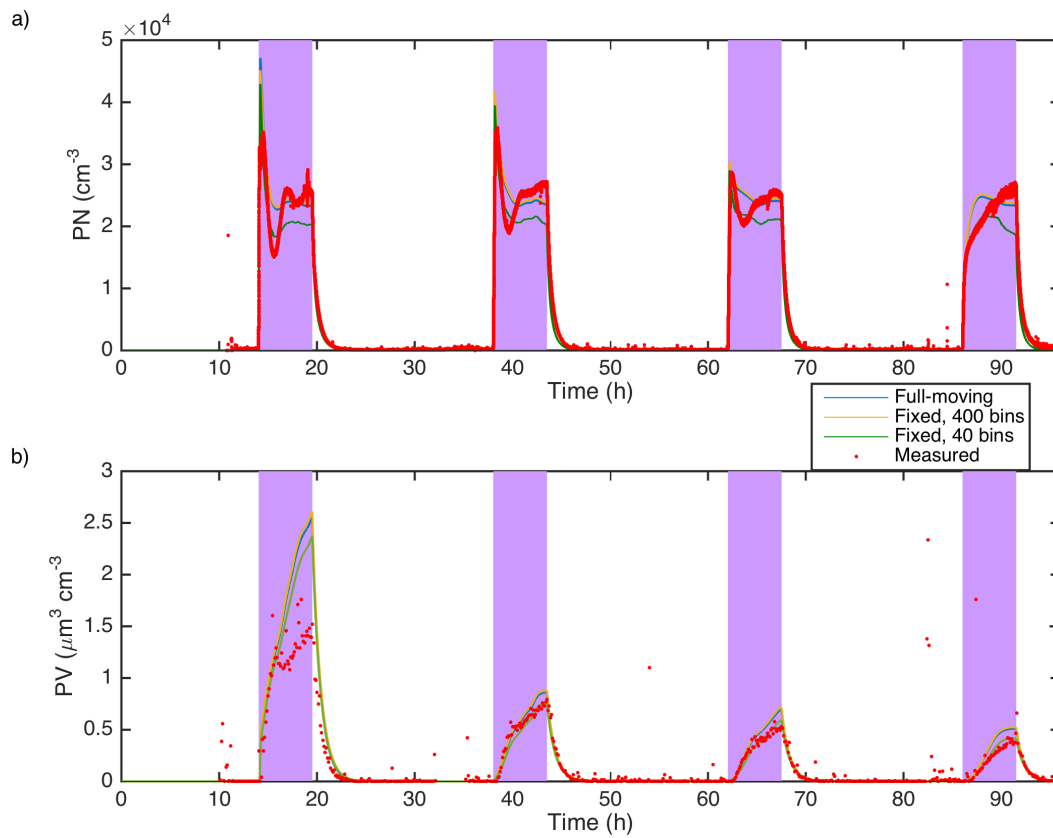


Figure S3. Modelled and measured total particle number concentration (a) and total particle volume concentration. The simulations were performed with the 2D-VBS. The only differences between the different model simulations are the size distribution method used (fixed sections or full-moving) and the number of size bins.

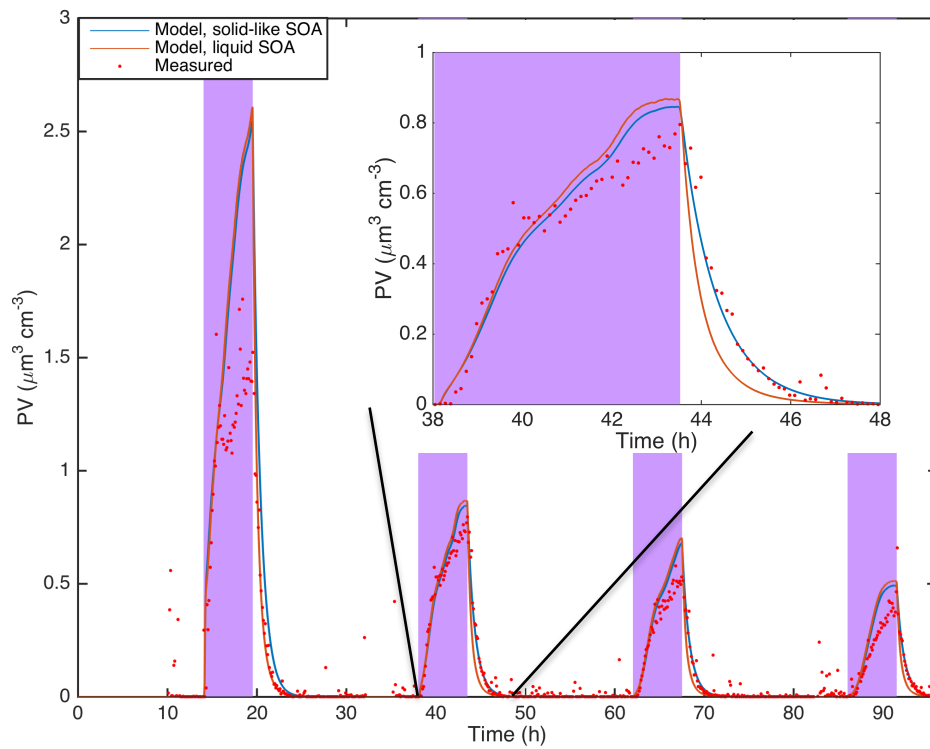


Figure S4. Modelled and measured total particle volume concentration. The simulations were performed with the 2D-VBS. The only differences between the different model simulations are the phase-state of SOA (solid-like or liquid).

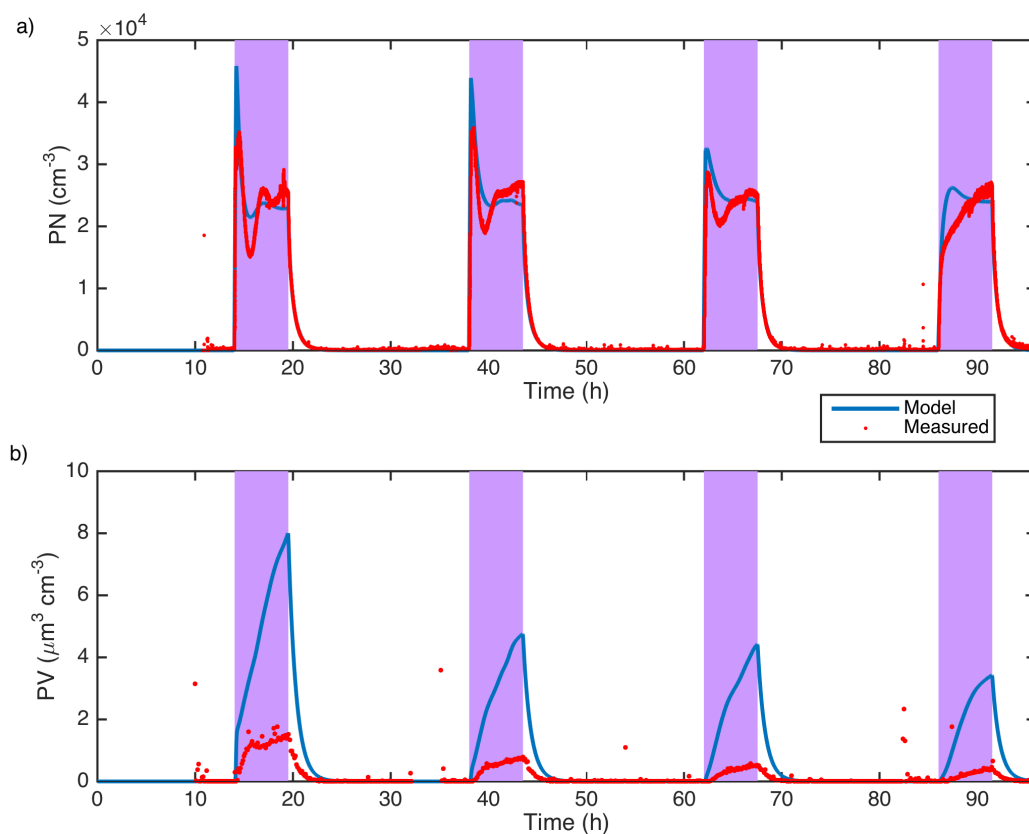


Figure S5. Modelled and measured (a) total particle number concentration and (b) total particle volume concentration. The model simulations were performed with the 2D-VBS using similar setup as was used in the original 2D-VBS parameterization from Jimenez et al. (2009) with $\gamma=1/6$, O:C equal to 0.4 for the first generation oxidation products, $k_{\text{OH}} = 3 \times 10^{-11} \text{ cm}^3 \text{ s}^{-1}$ and the compounds that fragmentize have equal probability to split at any of the carbon bonds.

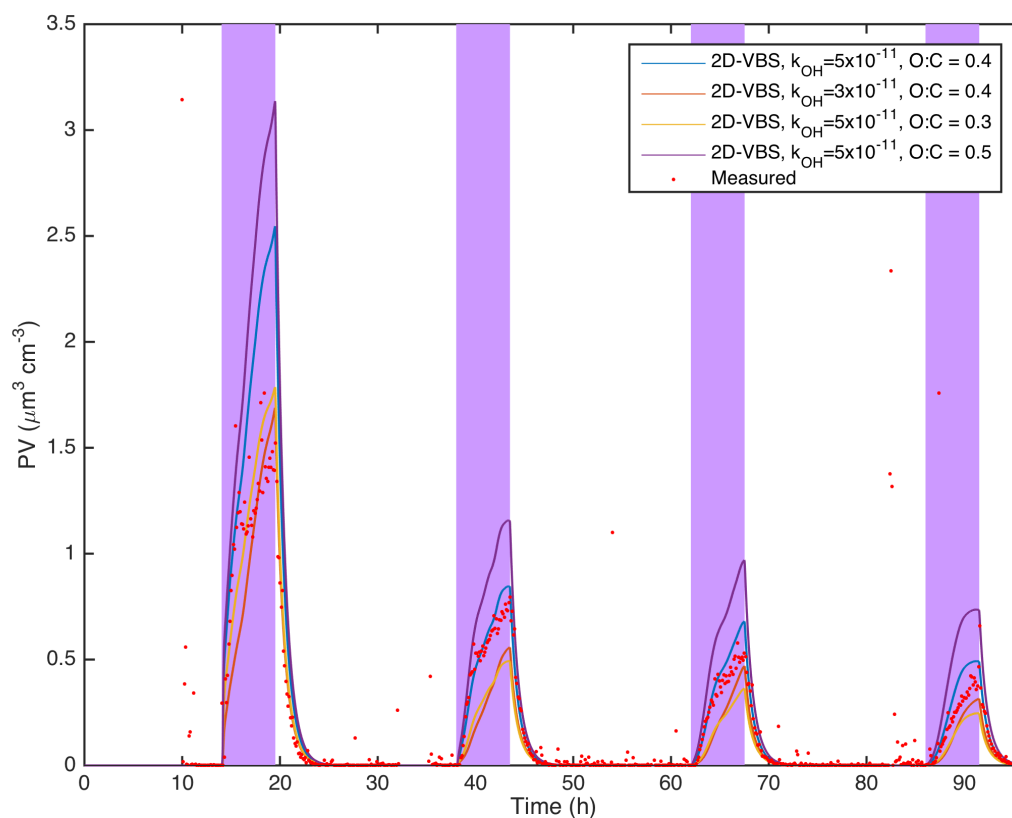


Figure S6. Modelled and measured total particle volume concentration. The model simulations were performed with the 2D-VBS and assuming that all fragmenting compounds fall into VBS-bins where C_{298}^* is at least 3 order of magnitude larger than the corresponding functionalization products and $\gamma=1/3$. O:C for the first generation oxidation products was varied in the range 0.3-0.5 and k_{OH} in the range 3×10^{-11} - 5×10^{-11} $\text{cm}^3 \text{s}^{-1}$.

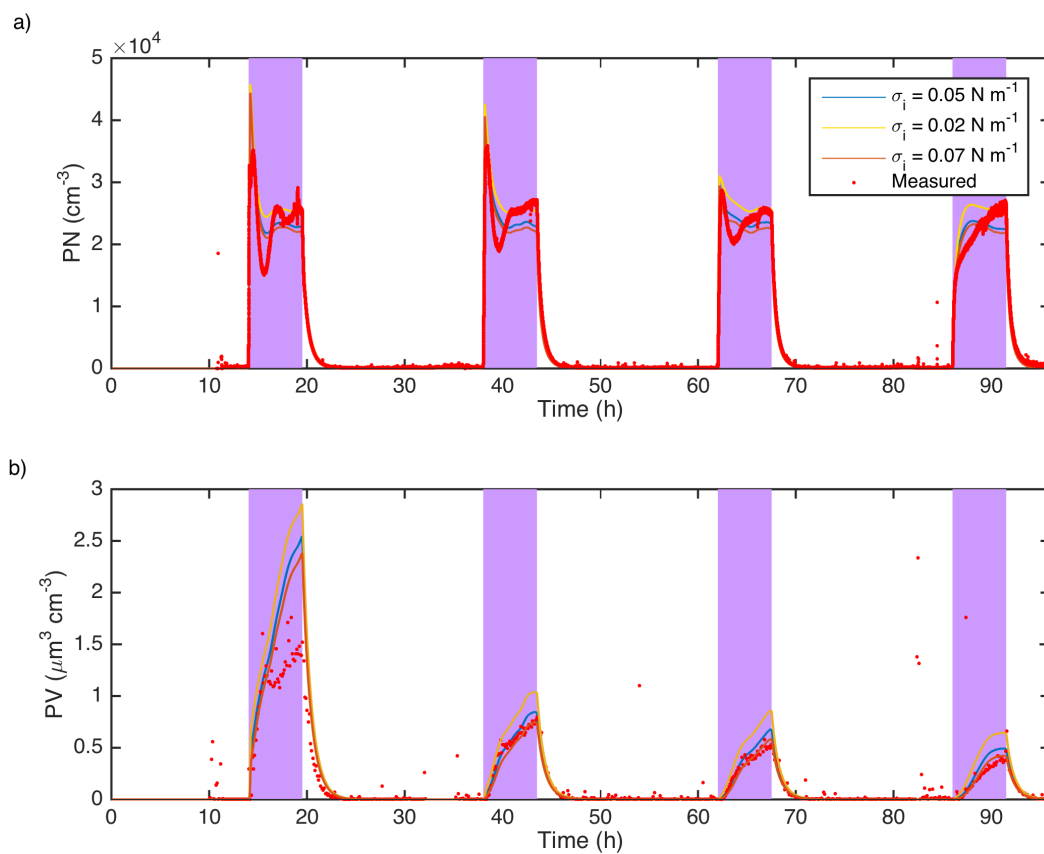


Figure S7. Modelled and measured (a) total particle number concentrations and (b) total particle volume concentrations. The model simulations were performed with the 2D-VBS. The only difference between the model simulations was the organic compound surface tension (σ_i).

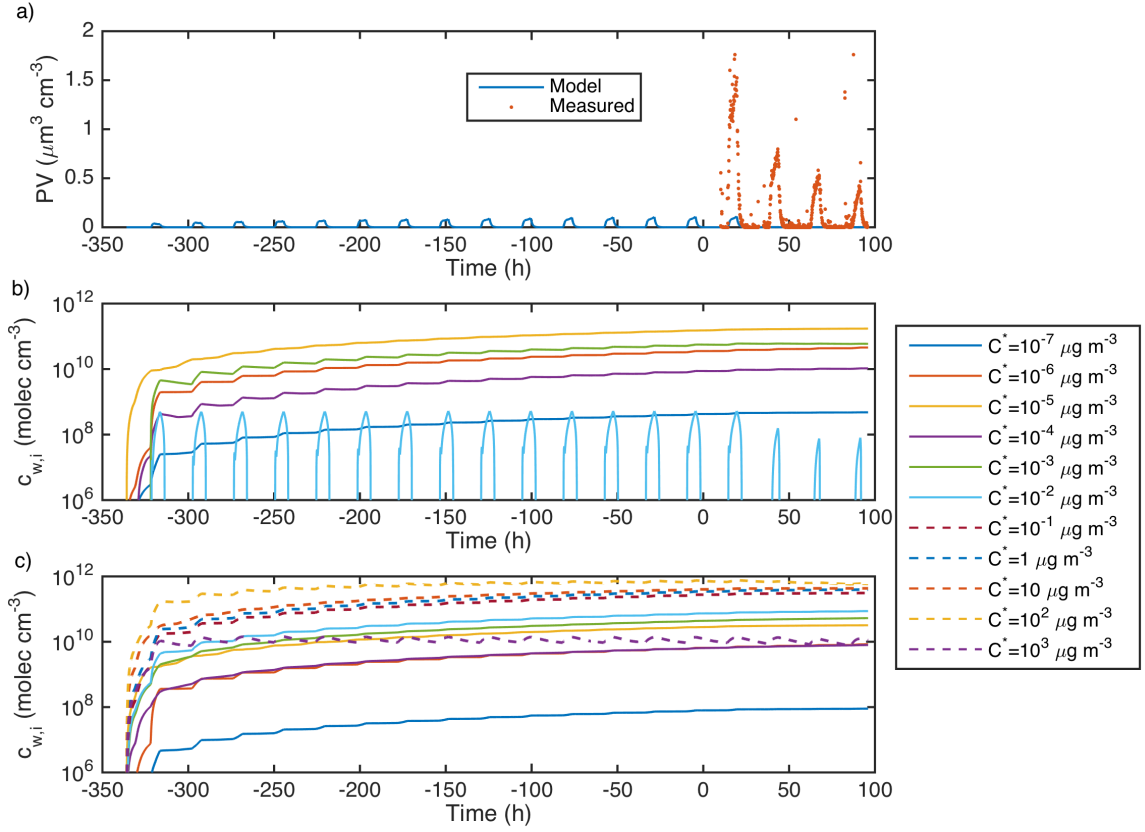


Figure S8. (a) Modelled and measured SOA volume formation and VOC wall uptake onto (b) the glass walls (Eq. 10-11) and (c) the PTFE Teflon walls when considering that the PTFE Teflon walls behave as FEB Teflon walls (Eq. 9, 12 and 13). The condensable organic compounds (in total 486 MCM compounds + 2 ELVOCs from α -pinene and Δ^3 -carene ozonolysis) have been grouped into different C^* bins. At time 0 h the intensive measurement campaign started. The ELVOCs formed from R1 are lumped into the volatility bin with $C^* = 10^{-5} \mu\text{g m}^{-3}$.

Based on the total VOC concentrations on the chamber walls (Fig. S8) and the assumption that the molecule radius (r_m) of the average VOC molecules is 0.3 nm and that the molecule cross section (σ_m) can be estimated as $r_m^2 \pi = 2.8 \times 10^{-19} \text{ m}^2$. We can estimate the maximum glass surface area covered by VOCs ($A_{m,glass}$) in the end of the experiments from Eq. S1. We then get a $A_{m,glass}$ 0.12 m^2 which is about 2 % of the total glass wall surface area in the chamber.

$$A_{m,glass} = V_{chamber} \sigma_m \sum_{i=1}^N (c_{w,glass,i}) \quad (\text{S1})$$

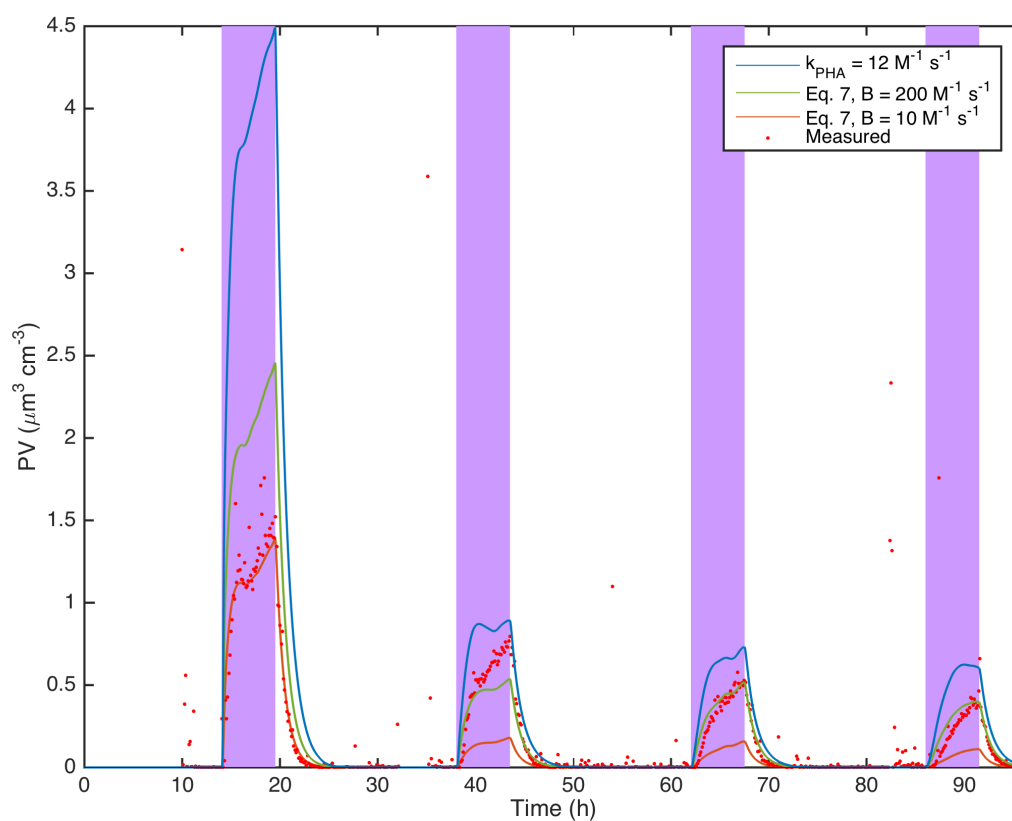


Figure S9. Modelled total particle volume concentration (PV). The model results are from simulations where the MCM compounds were used as condensable organic compounds and PHA formation was included using Eq. 7 with $B = 10 \text{ M}^{-1} \text{ s}^{-1}$ or $B = 200 \text{ M}^{-1} \text{ s}^{-1}$, and from a simulation with $k_{\text{PHA}} = 12 \text{ M}^{-1} \text{ s}^{-1}$.

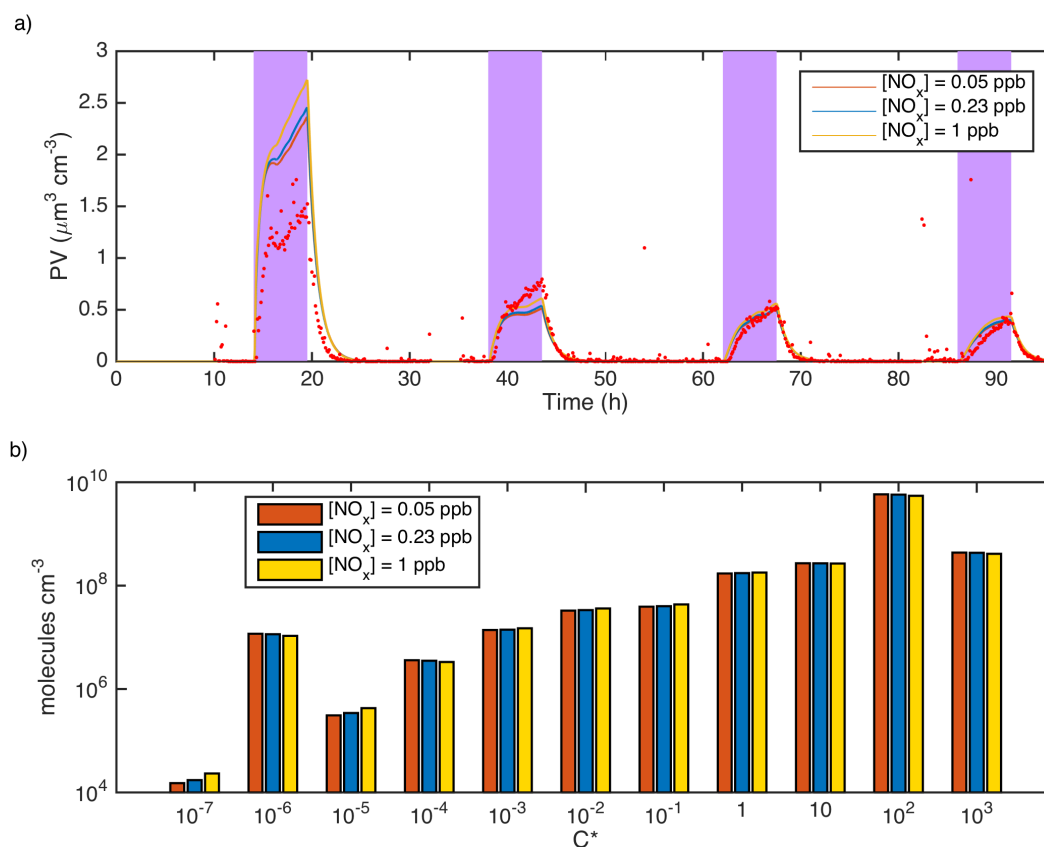


Figure S10. Modelled (a) total particle volume concentrations and (b) volatility distribution of the VOCs in the gas-phase during Day-3 and after 5 hours with UV-light on. The model results are from simulations where the MCM compounds were used as condensable organic compounds and PHA formation was included using Eq. 7 and $B = 200 \text{ M}^{-1} \text{ s}^{-1}$. The only difference between the different model simulations was the concentrations of NO_x in the inflow to the chamber.

References

Atkinson, R., Hasegawa, D., and Aschmann, S. M.: Rate Constants for the Gas-Phase Reactions of O_3 with a Series of Monoterpenes and Related Compounds at $296 \pm 2 \text{ K}$, *Int. J. Chem. Kinet.*, 22, 871-887, 1990.

Atkinson, R.: Gas-Phase Tropospheric Chemistry of Volatile Organic Compounds: 1. Alkanes and Alkenes, *Journal of Physical and Chemical Reference Data* 26, 215-290, doi: 10.1063/1.556012, 1997.

Atkinson, R., and Aschmann, S. M.: OH Radical Reaction Rate Constants for Polycyclic

Alkanes: Effects of Ring Strain and Consequences for Estimation Methods, *Int. J. Chem. Kinet.*, 24, 983-989, 1992.

Bowman, J. H., Barket, D. J., and Shepson, P. B.: Atmospheric Chemistry of Nonanal, *Environ. Sci. Technol.*, 37, 2218-2225, 2003.

Canosa-Mas, C. E., Duffy, J. M., King, M. D., Thompson, K. C, and Wayne, R. P.: The atmospheric chemistry of methyl salicylate—reactions with atomic chlorine and with ozone, *Atmospheric Environment*, 36, 2201-2205, 2002.

Coeur, C., Jacob, V., Foster, P., and Baussand, P.: Rate Constant for the Gas-Phase Reaction of Hydroxyl Radical with the Natural Hydrocarbon Bornyl Acetate, *Int. J. Chem. Kinet.*, 30: 497–502, 1998.

Corchnoy, S. B., and Atkinson, R.: Kinetics of the gas-phase reaction of hydroxyl and nitrogen oxide (NO₃) radicals with 2-carene, 1,8-cineole, p-cymene, and terpinolene, *Environ. Sci. Technol.*, 24, 1497-1502, 1990.

Jenkin, M. E., Saunders, S. M., and Pilling, M. J.: The tropospheric degradation of volatile organic compounds: a protocol for mechanism development, *Atmos. Environ.*, 31, 81–104, 1997.

Jenkin, M. E., Wyche, K. P., Evans, C. J., Carr, T., Monks, P. S., Alfarra, M. R., Barley, M. H., McFiggans, G. B., Young, J. C., and Rickard, A. R.: Development and chamber evaluation of the MCM v3.2 degradation scheme for β -caryophyllene, *Atmos. Chem. Phys.*, 12, 5275–5308, doi:10.5194/acp-12-5275-2012, 2012.

Pollmann, J., Ortega, J, and Helmig, D.: Analysis of Atmospheric Sesquiterpenes: Sampling Losses and Mitigation of Ozone Interferences, *Environ. Sci. Technol.*, 39, 9620-9629, 2005.

Saunders, S. M., Jenkin, M. E., Derwent, R. G., and Pilling, M. J.: Protocol for the development of the Master Chemical Mechanism, MCM v3 (Part A): tropospheric degradation of nonaromatic volatile organic compounds, *Atmos. Chem. Phys.*, 3, 161–180, doi:10.5194/acp-3-161-2003, 2003.

Zhang, X., Schwantes, R. H., McVay, R. C., Lignell, H., Coggon, M. M., Flagan, R. C., and Seinfeld, J. H.: Vapor wall deposition in Teflon chambers, *Atmos. Chem. Phys.*, 15, 4197-4214, doi:10.5194/acp-15-4197-2015, 2015.